





A kinetic model of the stress-induced void evolution in pentagonal whiskers and rods

A.S. Khramov ¹, S.A. Krasnitskii ² ✉, A.M. Smirnov ¹, M.Yu. Gutkin ^{1,3,4}

¹ ITMO University, St. Petersburg, Russia

² St. Petersburg State University, St. Petersburg, Russia

³ Peter the Great St. Petersburg Polytechnic University, St. Petersburg, Russia

⁴ Institute for Problems in Mechanical Engineering, Russian Academy of Sciences, St. Petersburg, Russia

✉ krasnitsky@inbox.ru

Abstract. A kinetic model of stress-induced vacancy diffusion in pentagonal whiskers and rods is suggested to investigate the void evolution there. In the framework of the model, the Gibbs-Thompson boundary conditions are employed to identify the free surface effect on the vacancy flux while the elastic fields of the wedge disclination are involved to reveal the contribution of the bulk effect. It is shown that the void evolution mode in the hollow pentagonal whiskers and rods is strongly determined by the initial internal and external radii as well as the materials parameters describing the response of both the residual stress and the surface tension. The void evolution diagram and kinetic curves are demonstrated to elucidate the critical and optimal parameters of this phenomenon.

Keywords: pentagonal whiskers; pentagonal rods; multiply twinned particles; residual stress; stress relaxation; disclination; hollow nanostructures; stress-induced diffusion

The article was prepared based on the report presented at the Symposium "Micromechanics of Functional Materials" at the XIII All-Russian Congress on Theoretical and Applied Mechanics.

Acknowledgements. This work was supported by the Russian Science Foundation (grant No. 22-11-00087, <https://rscf.ru/en/project/22-11-00087/>).

Citation: Khramov AS, Krasnitskii SA, Smirnov AM, Gutkin MY. A Kinetic Model of the Stress-Induced Void Evolution in Pentagonal Whiskers and Rods. *Materials Physics and Mechanics*. 2023;51(7): 22-33. DOI: 10.18149/MPM.5172023_4.

Introduction

Pentagonal crystal (PC) structures are deemed to be essential for enhanced performance in photonic, plasmonic and catalytic applications [1,2]. Their properties, prescribed not only by {111} faceting but also by cyclic twinning, evince more effective performance than their single-crystal analogs [3–5]. For most PCs such as pentagonal whiskers (PWs) or rods [6], plates [7], and decahedral particles (DhPs) [8], the five-fold cyclic twinning is common. The more complex multiply cyclic twinning corresponds to the class of icosahedral particles (IcPs) [9]. Besides, the cyclic twinning is responsible for inhomogeneous residual stress-strain states in PCs that significantly impact upon their functional properties [10–12].

Recently, much attention has been focused on the fabrication of hollow PC structures with tunable properties [13–17]. The fact that the hollowing process in PCs is strongly affected

by the residual stress caused by multiply twinning has been demonstrated in series of experiments [18–21]. For instance, Romanov et al. [18] observed voids in large CdTe PWs with diameter 1–10 mm. Later Yasnikov and Vikarchuk [19] employed the electrodeposition technique to produce both hollow and solid Cu PCs to investigate the size effect in the void formation. They observed the voids in relatively large PCs, while relatively small PCs remained free of voids. These experiments were explained by the higher level of the strain energy stored by the inhomogeneous residual stress in the larger PCs. Another example of stress-induced process of hollowing was described by Lu et al. [20] investigating the galvanic replacement reaction of both single-crystalline and multiply twinned Ag nanoparticles with HAuCl_4 in organic medium. The authors demonstrated that, under the galvanic replacement process, the single-crystalline Ag nanocubes evolved into nanoboxes while the multiply twinned Ag nanoparticles evolved into either pentagonal nanorings or nanocages of decahedral and icosahedral shapes. Similar results were obtained by Huang et al. [21] in examining the void growth phenomenon in single-crystalline and multiply twinned Pd nanoparticles placed in the Cu-acetylacetonate atmosphere. The authors reported that they synthesized hollow PdCu alloyed particles from the multiply twinned precursors in contrast to the void-free Pd/Cu core-shell particles produced from the single-crystalline precursors. Thus, to control the void evolution in PCs, it is essential to incorporate the residual stress effects into both the synthesis protocols and theoretical modeling.

The residual stress in PCs can be described within the disclination concept [22–24]. According to this concept, PWs and DhPs are considered as elastic bodies containing a positive partial wedge disclination with strength ~ 0.128 rad, while IcPs as elastic spheres containing a Marks-Ioffe stereo disclination with strength ~ 0.0613 sr that models the presence of six positive partial wedge disclinations with strength ~ 0.128 rad. It is worth noting that, within the disclination concept, various stress relaxation phenomena in PCs such as dislocation generation [25,26], crack initiation [27], formation of the phase inhomogeneities [28] and the misfit layers [29] has received the theoretical description in [30–35]. The phenomenon of the void evolution in the PCs has been elucidated in the large volume of the theoretical works as well.

Historically, the theoretical research concerning the void evolution phenomenon in PCs has focused on the interaction of point defects with wedge disclinations. The stress-induced diffusion of vacancies in vicinity of wedge disclinations was elucidated in the pioneer works [36–38].

Latter Mikhailin and Romanov [39] employed an elastic model and a molecular dynamic simulation to investigate the bulk vacancy migration to the disclination core placed in the center of a circular crystal plate. The numerical simulation demonstrated that the initial amorphization of the disclination core occurs and subsequently results in the nucleation of a cavity. Besides, it was revealed that incorporating the surface effects in the energy balance of the elastic plate leads to appropriate agreement with computer simulation results for the cavity formation phenomenon.

Romanov and Samsonidze [40] suggested a kinetic model of the point defects diffusion driven by the stress state of a wedge disclination in an elastic cylinder. The disclination core was considered as a perfect sink for point defects while the cylinder surface as a perfect source of them. The original profile of the point defects concentration inside the body was presumed to be relevant to the elastic disturbance of the disclination to introduce the initial and boundary conditions. The asymptotic expression for the point defects diffusion flux toward the disclination core was obtained in two limiting cases of (i) the initial stage, when the absorption of point defects in vicinity of the disclination prevails, and (ii) the final stage, when the steady-state condition is achieved.

Osipov and Ovid'ko [41] investigated the migration of substitutional atoms to triple junction disclinations in alloyed materials. The concentration of substitutional atoms in vicinity of a disclination core was derived with the assumption of the parabolic growth. It was inferred

that the split of the disclination, which was induced by the diffusion process, is one of the main factors responsible for the growth of a nucleus of amorphous phase under mechanical alloying.

Nazarov [42] analyzed the grain boundary diffusion affected by triple junction disclinations. He demonstrated that the stress gradients, induced by the disclination configurations, may explain anomalously high values of grain boundary diffusivity in nanocrystalline materials. To better understand the effects of a disclination on the grain boundary diffusion, Murzaev and Nazarov [43,44] implemented the molecular dynamic simulation of the grain boundary containing a partial disclination. They showed that the numerically calculated grain boundary diffusivity in disclinated nanocrystalline materials is at least two orders higher than in the disclination-free polycrystals.

Romanov et al. [18] examined the void formation in PWs and IcPs as a channel of residual stress relaxation. Within the quasi-equilibrium energetic approach, the critical conditions of a void formation in PCs were determined in terms of the change of surface and disclination strain energies due to the void growth. Using the stress fields of wedge disclinations in elastic bodies with spherical surfaces that were found by Kolesnikova et al. [45], Krasnitckii et al. [46] later considered a similar problem for DhPs. In spite of the fact that the energetic approach has quite limited applications (as it does not include the kinetic aspects of the problem), the optimal size of voids prescribed by the stress relaxation models in [18,46] is in agreement with experimental observations of hollow PCs [18,19].

Vlasov et al. introduced the most thorough formulation of non-steady stress-induced diffusion problems concerning the formation of impurity atmospheres in vicinity of triple junction disclinations [47,48] as well as the growth of void and phase nuclei in PWs [49,50] and IcPs [51,52]. For the case of void growth in PWs, Vlasov et al. [49] managed to derive the strict analytical solutions for the void radius rate. Besides, it was demonstrated [52] that, at the initial stage, when the disturbance induced by the body external surface is negligible, the nucleus radius rate in vicinity of wedge and stereo disclinations varies as $\sim t^{1/2}$ (hereinafter t is the time of the process) in contrast to that in vicinity of edge dislocations and tips of mode I cracks, varying as $\sim t^{1/3}$ and $\sim t^{2/5}$, respectively.

Later Tsagrakis et al. [53] considered the void growth phenomena in IcPs with accounting for size effects within the gradient elasticity theory. The gradient solution for a stereo disclination was found to provide nonsingular profiles of the vacancy velocity and the vacancy concentration inside IcPs. The authors showed that the gradient elastic effects are essential to consider when the internal length parameter is of the same order of magnitude as the particle radius, otherwise these effects can be neglected.

It is worth noting that the aforementioned kinetics models have a serious limitation. In fact, they are unable to incorporate the influence of surface tension in the void evolution process in PCs. Recently Krasnitckii et al. [54] have overcome this limitation by involving the surface tension on the inner and outer surfaces of hollow IcPs in the form of the linearized Gibbs-Tompson conditions. The corresponding stress-assisted diffusion problem under the steady-state approximation was solved to consider the void evolution kinetics driven by both the surface and bulk stress effects. It was shown that the void evolves in either the shrinking mode, if the vacancy flux induced by the Gibbs-Tompson effects is predominant, or the growing mode, if the pressure-induced vacancy flux prevails, or the stabilizing mode, if the contributions of these fluxes are equal.

The present work is aimed at extending the general formalism of the model suggested in [54] to investigate the stress-induced vacancy diffusion as well as the void evolution phenomena in PWs under the Gibbs-Tompson curvature effects. It represents (i) a solution of the steady-state problem of vacancy diffusion for a hollow cylindrical body, (ii) an analysis of the void evolution kinetics in a PW, and (iii) an evaluation of the critical and optimal parameters of the void equilibrium state.

Model

Consider a hollow PW as a long hollow cylindrical body containing a positive partial wedge disclination of strength $\omega \approx 0.128$ rad (Fig. 1(a)). The wedge disclination is responsible for the hydrostatic compression in the inner region of the cylinder and for the hydrostatic tension in its outer region. This volumetric strain stimulates both the generation of vacancies at the stretched surface of the PW and subsequent migration of the vacancies inward the compressed region, where they can coagulate with formation of a central cylindrical void. The stress-assisted vacancy diffusion can be described by the second Fick law with a drift term [54]:

$$\frac{1}{D} \frac{\partial C}{\partial t} = \Delta C + \frac{1}{kT} \nabla C \cdot \nabla W_{int} + \frac{C}{kT} \Delta W_{int}, \quad (1)$$

where C is the relative (dimensionless) concentration of vacancies inside the cylinder, D is the diffusivity of vacancies, k is the Boltzmann constant, T is the absolute temperature, $W_{int} = P \delta v$ is the interaction energy of a vacancy with the wedge disclination, P is the hydrostatic pressure exerted by the wedge disclination stress tensor σ ($P = -1/3 \text{tr } \sigma$), and δv is the vacancy relaxation volume ($\delta v < 0$). The hydrostatic pressure P reads [24]:

$$P = -\frac{G\omega}{3\pi} \frac{1+\nu}{1-\nu} \left[\frac{1}{2} + \ln \frac{r}{a} + \frac{a_v^2}{a^2 - a_v^2} \ln \frac{a_v}{a} \right], \quad (2)$$

where G is the shear modulus, ν is the Poisson coefficient, a_v and a are the internal and external radii, respectively, of the hollow cylinder, and r is the radial coordinate.

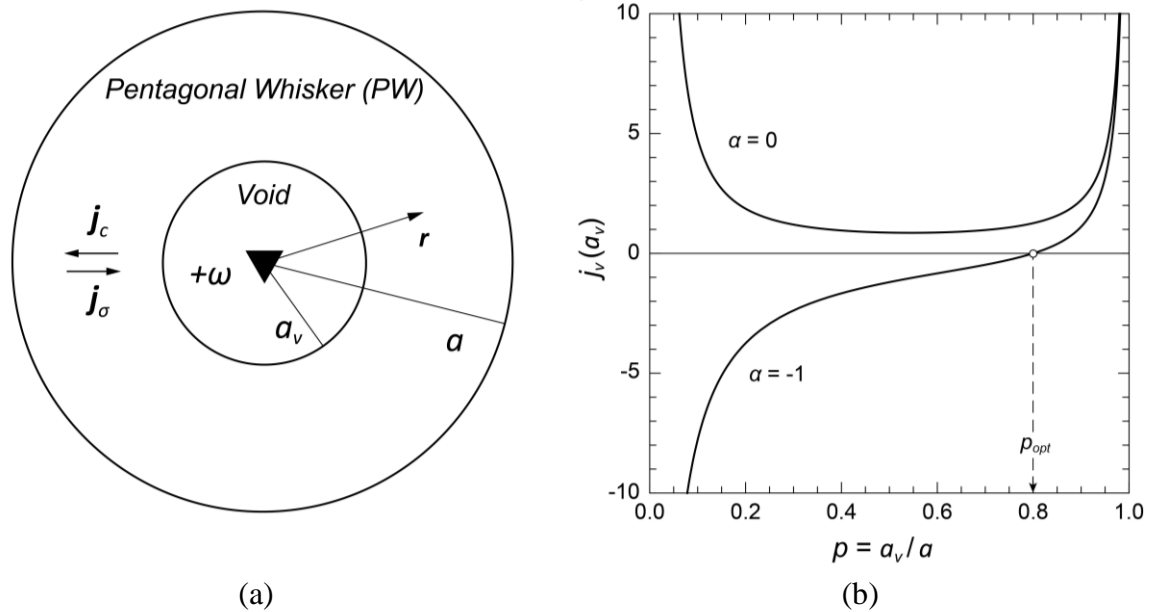


Fig. 1. (a) Continuum model of a PW with a central cylindrical void. (b) The radial flux of vacancies $j_v(a_p)$ through the void surface in dependence of the normalized void radius p for $\alpha = 0$ (single-crystalline tubes) and $\alpha = -1$ (PWs). The radial flux is given in units of $C_0 D / \Omega$

Substituting Eq. 2 in the diffusion equation Eq. 1, for the steady-state process ($\partial C / \partial t \approx 0$) in the case of the cylindrical symmetry, one can come to the following equation:

$$\frac{d^2 C}{dr^2} + \frac{1-\alpha}{r} \frac{dC}{dr} = 0, \quad (3)$$

where α is the dimensionless complex which defines the disclination stress contribution to the diffusion process:

$$\alpha = \frac{G\omega}{3\pi} \frac{1+\nu}{1-\nu} \frac{\delta v}{kT}. \quad (4)$$

In addition to the bulk effects accompanying the void growth in PWs, the surface effects viz. surface tension should be also taken into consideration. Actually, the surface tension produces a negative pressure (positive hydrostatic stress) on the inner surface while the outer surface is affected by a positive pressure (negative hydrostatic stress). From this point of view, the vacancy concentration at the inner surface can be bigger than at the outer one. It means that the vacancy flux inside PWs can be either inhibited or even inversed by the surface tension. The latter phenomenon exerts the void shrinking with its subsequent collapse. The impact of the surface tension on the void evolution can be taken into account in the linearized form of the Gibbs-Thompson boundary conditions as follows [55]:

$$C|_{r=a_p} = C_0 \left(1 + \frac{\beta}{a_v}\right), \quad C|_{r=a_p} = C_0 \left(1 - \frac{\beta}{a}\right), \quad (5a,b)$$

where C_0 is the equilibrium concentration of vacancies near the flat surface, $\beta = \gamma\Omega/(kT)$ is the length parameter, γ is the specific surface energy, Ω is the atomic volume.

The solution of the diffusion equation (Eq. 3) with regard to the boundary conditions (Eqs. 5) is given by

$$C = C_0 \left(1 + \beta \frac{a(a^\alpha - r^\alpha) - a_v(r^\alpha - a_v^\alpha)}{a a_v (a^\alpha - a_v^\alpha)}\right). \quad (6)$$

It is worth noting that Eq. 6 coincides with the solution of the diffusion problem for the defect-free cylindrical shells given in [55], if the parameter α tends to zero.

Results

The void evolution phenomenon in hollow PWs is strongly determined by the migration of vacancies. Inside the PWs, the migration of vacancies can be described in terms of the radial flux as follows:

$$j_v = j_c + j_\sigma, \quad (7)$$

where j_c is the vacancy flux caused by the vacancy concentration gradient between the inner and outer surfaces of the PWs,

$$j_c = -\frac{D}{\Omega} \nabla C, \quad (8)$$

and j_σ is the stress-induced vacancy flux caused by the elastic field of the wedge disclination,

$$j_\sigma = -\frac{D}{\Omega} \frac{C}{kT} \nabla W_{int}. \quad (9)$$

The radial vacancy flux in Eq. 7 can be rewritten with respect to the concentration profile (given by Eq. 6) in the following form:

$$j_v(r) = \frac{\alpha C_0 D}{\Omega} \frac{(a_v + \beta)a^{1+\alpha} - (a - \beta)a_v^{1+\alpha}}{a a_v (a^\alpha - a_v^\alpha) r}. \quad (10)$$

To investigate the void evolution phenomenon, one can consider the dependencies of the radial vacancy flux through the inner surface $j_v(a_v)$ on the radii ratio $p = a_v/a$ shown in Fig. 1(b) for different values of α . The void evolution mode is defined by the sign of the total vacancy flux at the void surface in Eq. 10. If the flux is negative, the inward stress-induced flux prevails so that vacancies are absorbed by the void, thus provoking the void growth mode. When the flux is positive, the outward concentration flux is predominant so that vacancy emission from the void evincing the void shrinkage mode is expected. Besides, if the vacancy flux turns to

zero, the contributions of the concentration and stress-induced fluxes are equal in magnitude so that the void gets an optimal size $p = p_{opt}$ evincing the equilibrium mode.

According to Fig. 1(b), the relatively small voids (when $p < p_{eq}$) in hollow PWs with $\alpha = -1$ tend to grow until reaching the optimal radius p_{opt} . On the contrary, the relatively large voids (when $p > p_{eq}$) tend to shrink to the optimal radius p_{opt} . In the case of defect-free single-crystalline tubes with $\alpha = 0$, the vacancy flux is positive for any radii ratio p , hence the void growth mode occurs to transform tubes into solid rods.

Since the void evolution mode in PWs is mainly determined by the sign of the vacancy flux at the void, one can derive the critical mode condition from the vanishing flux equation $j_v(a_v) = 0$ in the form:

$$\frac{a_v + \beta}{a - \beta} = \left(\frac{a_v}{a} \right)^{\alpha+1}. \quad (11)$$

Introducing dimensionless variables, one can rewrite Eq. 11 with regard to the mass conservation law [54], $a^2 - a_v^2 = a_0^2$, as follows:

$$\alpha = \log_p \frac{p b_0 + \Delta}{p(b_0 - \Delta)}, \quad (12)$$

where $p = a_v / a$, $\Delta = (1 - p^2)^{1/2}$, $b_0 = a_0 / \beta$, and a_0 is the radius of a solid PW.

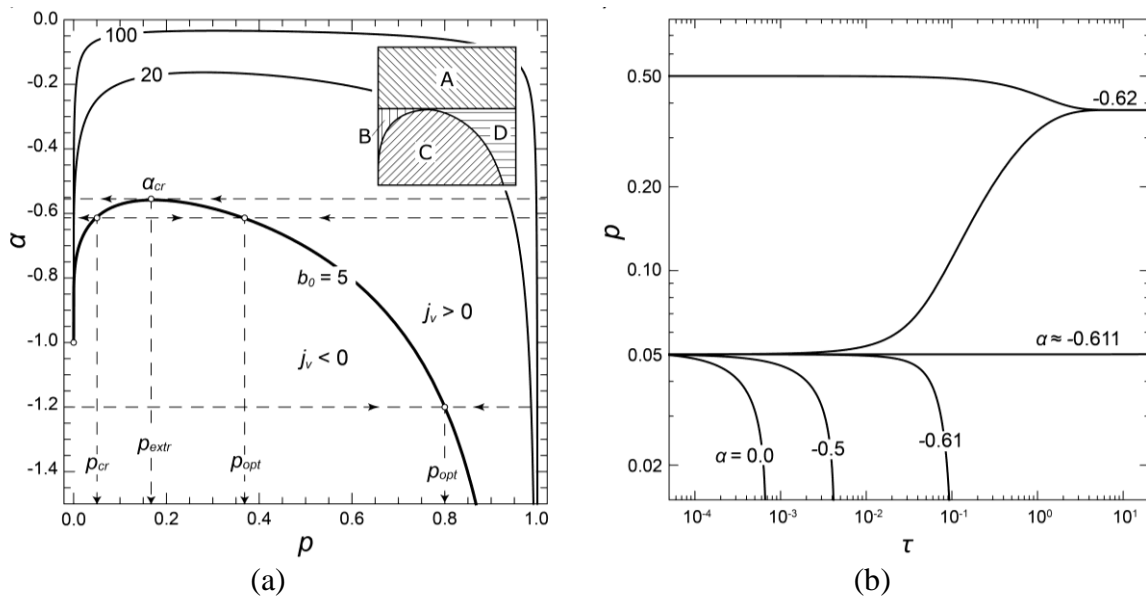


Fig. 2. (a) Dependence of the parameter α on the normalized void radius p for different values of $b_0 = 5, 20$ and 100 . The inset in the upper right corner indicates the regions A, B, C and D corresponding to different scenarios of void evolution. (b) Dependence of the normalized void radius p on the dimensionless time τ given for different values of the initial void radius $p_0 = 0.05$ and 0.5 , and the parameter $\alpha = 0.0, -0.5, -0.61, -0.62$, and $\alpha \approx -0.611$

Figure 2(a) demonstrates the curves $\alpha = f(p)$ given by Eq. 12 for different values of the parameter $b_0 = 5, 20$ and 100 . These curves define the parameters α and p of hollow PWs for which $j_v(a_v) = 0$, i.e. the void equilibrium mode takes place. The area below the curves ($\alpha < f(p)$) corresponds to the void growth mode when $j_v(a_v) < 0$, while the area above them ($\alpha > f(p)$) to the void shrinkage mode when $j_v(a_v) < 0$. It is worth noting that the area above curves reduces if the parameter b_0 increases.

The void evolution scenarios in the hollow PWs are determined by the roots of the equation $\alpha = f(p)$ for a given value of α (see Fig. 2(a)). For example, the equation $\alpha = f(p)$ has

no roots for $\alpha_{cr} < \alpha \leq 0$ so the void shrinkage mode is valid for any p , and hence the void of any

size is unstable. For $\alpha = \alpha_{cr}$, there is the only root $p = p_{extr}$ corresponding to the unstable equilibrium state of the void, i.e. any perturbation of its radius results in the transition to the shrinkage mode. The cases of $p = p_{cr}$ and $p = p_{opt}$ can be elucidated as the unstable and stable equilibrium void states, respectively. For $\alpha < -1$, the equation $\alpha = f(p)$ has the only one root, $p = p_{opt}$, relating to the stable equilibrium state of the void. To obtain the stable equilibrium, the voids with p from the range of $0 < p < p_{opt}$ must grow, while those with p from the range of $p_{opt} < p < 1$ must shrink.

Thus, the voids in PWs should be unstable and have a tendency to shrinkage if either $\alpha_{cr} < \alpha \leq 0$ for any void radius (see region A in Fig. 2(a)) or $-1 \leq \alpha < \alpha_{cr}$ for pre radius less than a critical one (see region B in Fig. 2(a)). In contrast, the stable void can evolve via either shrinkage or growth if $\alpha < -1$ for any void radius and $-1 \leq \alpha < \alpha_{cr}$ for void radius larger than the critical value (see regions C and D in Fig. 2(a)).

Turning now to the kinetic aspects of the void evolution in hollow PWs, the growth rate is defined by the vacancy flux at the void surface:

$$\frac{da_v}{dt} = -\Omega j_v(a_v). \quad (13)$$

The Eq. 13 can be derived as follows:

$$\frac{dp}{d\tau} = -\frac{\alpha \Delta^4 (1 - \Delta/b_0) p^{1+\alpha} - (p + \Delta/b_0)}{p^2 (1 - p^\alpha)}, \quad (14)$$

where $\tau = C_0 D t / a_0^2$ is the dimensionless time.

The numerical solution of the void evolution equation (Eq. 14) is illustrated in Fig. 2(b) for $b_0 = 5$ (in this case, $\alpha_{cr} \approx -0.558$, see Fig. 2(a)). According to Fig. 2(b), for the given initial normalized radius $p_0 = 0.05$ of the void, some different scenarios of its evolution can occur. For $\alpha = 0.0$ and $-0.5 (> \alpha_{cr} \approx -0.558)$, the void tends to shrink with subsequent collapse (see region A in Fig. 2(a)). Similar pathway is expected in the case when $\alpha = -0.61 (< \alpha_{cr} \approx -0.558)$ and the initial radius p_0 of the void is less than critical value $p_{cr} \approx 0.051$ (region B). Moreover, the time for the void collapse is mainly determined by α : the smaller the value of α , the longer the void shrinking process. As is seen from Fig. 2(b), for even smaller $\alpha = -0.62$, the void tends to take the optimal size via either its growth (for $p_0 = 0.05$ corresponding to region C) or shrinkage (for $p_0 = 0.5$ corresponding to region D). It is worth noting that, for $\alpha \approx -0.611$, the normalized radius $p_0 = 0.05$ of the void coincides with the critical one, p_{cr} , so the void occurs in the state of unstable equilibrium when any perturbation of its radius causes either shrinking or growing.

Let us now examine the critical and optimal conditions of the void evolution process in PWs. As was mentioned above, the nucleation of stable voids in solid PWs is possible if the absolute value of parameter α exceeds that of some critical value α_{cr} only. The latter one strongly depends on the ratio of the solid PW radius a_0 to the length parameter β . The parameter α characterizes the bulk effects in solid PWs attributed to the wedge disclination stress while the parameter β describes the role of surface effects (the bigger the surface energy γ the bigger β). Fig. 3(a) illustrates the dependence of α_{cr} on the solid PW radius a_0 for different values of the length parameter $\beta = 5, 10, \text{ and } 20$ nm. As is seen from Fig 3(a), the critical value α_{cr} first sharply increases for $0 < a_0 < 200$ nm and then gradually tends to zero for $a_0 > 200$ nm. Besides, for a given value of the solid PW radius a_0 , the critical value α_{cr} decreases with an increase in β . It means that, in PWs of the same size (for example, at $a_0 = 100$ nm), the void nucleation is more likely to occur in the PWs with smaller surface tension ($\alpha_{cr} \approx -0.15$ for $\beta = 5$ nm whereas $\alpha_{cr} \approx -0.55$ for $\beta = 20$ nm).

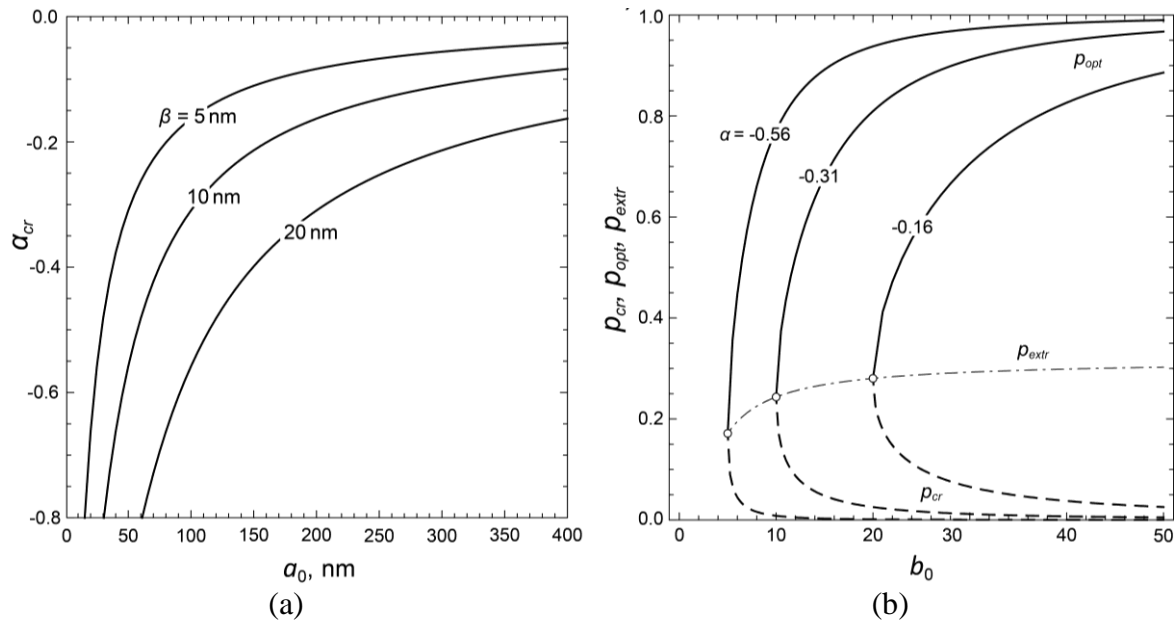


Fig. 3. (a) Dependence of the critical value α_{cr} on the solid PW radius a_0 for different values of the parameter $\beta = 5, 10$ and 20 nm. (b) The dependences of the normalized void radii p_{cr} (solid curves), p_{opt} (dashed curves), and p_{extr} (dashed-and-dotted curve) on the dimensionless parameter b_0 for $\alpha = -0.16, -0.31, \text{ and } -0.56$

In contrast to the case of $\alpha_{cr} < \alpha \leq 0$, when the void initiation failed, the barrier-controlled nucleation of voids in solid PWs can occur if the normalized radius of void nucleus exceeds its critical value p_{cr} at $-1 \leq \alpha < \alpha_{cr}$. In this case, the void nucleus tends to grow until it reaches the optimal size and $p = p_{opt}$. As it was mentioned above, the values of parameters p_{cr} and p_{opt} are strongly determined by the material parameters α and $b_0 = a_0 / \beta$ demonstrating the role of size effect in the void evolution phenomenon. The dependences of the characteristic normalized radii of voids in PWs, p_{cr} , p_{extr} , and p_{opt} , on the value of b_0 are shown in Fig. 3b for different values of α . As is seen from Fig. 3(b), the critical and optimal normalized radii coincide with the extremal value p_{extr} if α takes the critical value. When b_0 increases, p_{cr} decreases while p_{opt} increases. In the limiting cases, when $\alpha \rightarrow -1$ or $b_0 \rightarrow +\infty$, the critical normalized radius of the void vanishes, the optimal one tends to 1.0 (the case of an infinitely thin-wall tube), and the extremal one tends to a constant value ~ 0.3 .

In the case of $\alpha < -1$, the barrier-less nucleation of voids in PWs should occur. Indeed, the contribution of the surface tension to void evolution is negligible with regard to the impact of the disclination stress field. As a result, the void nucleus is expected to grow in order to take a stable state with its optimal normalized radius p_{opt} .

Conclusions

In summary, the void evolution kinetics in PWs has been reconsidered with regard to the curvature surface effect. In doing so, the linearized Gibbs-Thompson boundary conditions are incorporated in the boundary-value problem of stress-assisted vacancy diffusion inside a hollow cylindrical body. It is shown that the vacancy flux is mainly determined by the dimensionless parameters α indicating the impact of the bulk stress state of the wedge disclination, and β describing the effect of the surface tension on the vacancy diffusion. With assuming that the direction of the vacancy flux completely prescribes the void shrinkage or growth modes in hollow PWs, various void evolution scenarios have been revealed with respect to the initial void radius $a_{v,0}$ and the dimensionless parameters α and $b_0 = a_0 / \beta$ (where a_0 is the radius of a

solid PW) which reflect the contributions of the bulk stress and surface effects, respectively, to the void evolution process.

According to the first scenario, in PWs with $\alpha_{cr} < \alpha < 0$, the void of any size is unstable, i.e. it tends to shrink with the subsequent collapse. Hence, the void nucleation is completely inhibited by the surface effects.

In PWs with $-1 \leq \alpha < \alpha_{cr}$, the voids of size smaller than a critical one are not stable and tend to shrink, in contrast to the voids of size larger than the critical one tend to reach the stable state with the optimal radius $a_{v,opt}$.

When $\alpha < -1$, the voids of any size have the tendency to reach the stable state via either growing (if $a_v < a_{v,opt}$) or shrinking (if $a_v > a_{v,opt}$). Hence, the bulk stress effect prevails and stimulates the void nucleation to occur.

Finally, the critical and optimal parameters of the void evolution scenarios are identified with respect to the bulk and surface effects. It is shown that the critical parameter α_{cr} increases with an increase in the solid PW radius a_0 as well as with a decrease in the length parameter β . That is the bigger the PW size the less the influence of the surface tension and hence the barrier for void nucleation. Besides, the critical radius of void nucleus $a_{v,cr}$ also declines with an increase in the solid PW size. As for the optimal radius $a_{v,opt}$ of a stable void, the rise of both the parameters b_0 and $|\alpha|$ leads to an increase in the optimal radius of the void. Moreover, in the limiting cases when $b_0 \rightarrow +\infty$ and $\alpha \rightarrow -\infty$, the hollow PWs could evolve in thin-wall pentagonal tubes.

One of the most significant findings to emerge from this model is that the surface effects such as surface tension is essential to incorporate in the problem of the void evolution in PWs if the material parameter $\alpha > -1$. When $\alpha < -1$, the surface effect on the void nucleation can be neglected.

References

1. Hamans RF, Parente M, Garcia-Etxarri A, Baldi A. Optical properties of colloidal silver nanowires. *The Journal of Physical Chemistry C*. 2022;126(20): 8703-8709.
2. Lyu Z, Shang Y, Xia Y. Shape-Controlled Synthesis of Copper Nanocrystals for Plasmonic, Biomedical, and Electrocatalytic Applications. *Accounts of Materials Research*. 2022;3(11): 1137-1148.
3. Carbo-Argibay E, Rodriguez-Gonzalez B. Controlled Growth of Colloidal Gold Nanoparticles: Single-Crystalline versus Multiply-twinned Particles. *Israel Journal of Chemistry*. 2016;56(4): 214-226.
4. Marks LD, Peng L. Nanoparticle shape, thermodynamics and kinetics. *Journal of Physics: Condensed Matter*. 2016;28(5): 053001.
5. Ji G, Ji A, Lu N, Cao Z. Formation and morphology evolution of icosahedral and decahedral silver crystallites from vapor deposition in view of symmetry misfit. *Journal of Crystal Growth*. 2019;518: 89-94.
6. Zhao H, Eggeman AS, Race CP, Derby B. Geometrical constraints on the bending deformation of Penta-twinned silver nanowires. *Acta Materialia*. 2020;185: 110-118.1
7. Yoo Y, Kim SI, Han S, Lee H, Kim J, Kim HS, Ahn JP, Kang T, Choo J, Kim B. Epitaxially aligned submillimeter-scale silver nanoplates grown by simple vapor transport. *Nanoscale*. 2019;11(37): 17436-17443.
8. Zhou S, Zhao M, Yang TH, Xia Y. Decahedral nanocrystals of noble metals: Synthesis, characterization, and applications. *Materials Today*. 2019;22: 108-131.
9. Wang H, Zhou S, Gilroy KD, Cai Z, Xia Y. Icosahedral nanocrystals of noble metals: synthesis and applications. *Nano Today*. 2017;15: 121-144.
10. Kuo CH, Lamontagne LK, Brodsky CN, Chou LY, Zhuang J, Sneed BT, Sheehan MK, Tsung CK. The effect of lattice strain on the catalytic properties of Pd nanocrystals. *ChemSusChem*. 2013;6(10): 1993-2000.

11. Mychinko M, Skorikov A, Albrecht W, Sánchez-Iglesias A, Zhuo X, Kumar V, Liz-Marzán L, Bals S. The Influence of Size, Shape, and Twin Boundaries on Heat-Induced Alloying in Individual Au@Ag Core–Shell Nanoparticles. *Small*. 2021;17(34): 2102348.
12. Huang J, Liu Q, Yan Y, Qian N, Wu X, Ji L, Li X, Li J, Yanga D, Zhang H. Strain effect in Pd@PdAg twinned nanocrystals towards ethanol oxidation electrocatalysis. *Nanoscale Advances*. 2022;4(1): 111–116.
13. Han L, Xiong P, Bai J, Che S. Spontaneous formation and characterization of silica mesoporous crystal spheres with reverse multiply twinned polyhedral hollows. *Journal of the American Chemical Society*. 2011;133(16): 6106–6109.
14. Huang H, Zhang L, Lv T, Ruditskiy A, Liu J, Ye Z, Xia Y. Five-Fold twinned Pd nanorods and their use as templates for the synthesis of bimetallic or hollow nanostructures. *ChemNanoMat*. 2015;1(4): 246–252.
15. Zhou X, Qi W, Li Y. Simple Synthesis of Ru Decahedral Hollow Nanocages with Face-Centered Cubic Structure. *Journal of Nanoscience and Nanotechnology*. 2021;21(10): 5302–5306.
16. Wang W, Shi Y, Chen Z, Zhao M, Cao Z, Lyu Z, Chen R, Xiao K, Chi M, Xia Y. Synthesis and Characterization of Pt-Ag Icosahedral Nanocages with Enhanced Catalytic Activity toward Oxygen Reduction. *ChemNanoMat*. 2022;8(9): e202200186.
17. Krasnitckii SA, Gutkin MY. Review on theoretical models of void evolution in crystalline particles. *Reviews on Advanced Materials and Technologies*. 2021;3(1): 96–126.
18. Romanov AE, Polonsky IA, Gryaznov VG, Nepijko SA, Junghanns T, Vitrykhovski NJ. Voids and channels in pentagonal crystals. *Journal of Crystal Growth*. 1993;129: 691–698.
19. Yasnikov IS, Vikarchuk AA. Voids in icosahedral small particles of an electrolytic metal. *Journal of Experimental and Theoretical Physics Letters*. 2006;83(1): 42–45
20. Lu X, Tuan HY, Chen J, Li ZY, Korgel BA, Xia Y. Mechanistic studies on the galvanic replacement reaction between multiply twinned particles of Ag and H₂AuCl₄ in an organic medium. *Journal of the American Chemical Society*. 2007;129(6): 1733–1742.
21. Huang J, Yan Y, Li X, Qiao X, Wu X, Li J, Shen R, Yang D, Zhang H. Unexpected Kirkendall effect in twinned icosahedral nanocrystals driven by strain gradient. *Nano Research*. 2020; 13: 2641–2649.
22. Wit RDe. Partial disclinations. *Journal of Physics. C. Solid State Physics*. 1972;5: 529–534.
23. Romanov AE, Kolesnikova AL. Application of disclination concept to solid structures. *Progress in Material Science*. 2009;54: 740–769.
24. Romanov AE, Kolesnikova AL. Elasticity Boundary-Value Problems for Straight Wedge Disclinations. A Review on Methods and Results. *Reviews on Advanced Materials and Technologies*. 2021;3(1): 55–95.
25. Saito Y. Crystal structure and habit of silicon and germanium particles grown in argon gas. *J. Cryst. Growth*. 1979;47(1): 61–69.
26. Chen Y, Huang Q, Zhao S, Zhou H, Wang J. Interactions between Dislocations and Penta-Twins in Metallic Nanocrystals. *Metals*. 2021; 11(11): 1775.
27. Yasnikov IS. On the problem of the formation of an open sector instead of a twin boundary in electrolytic pentagonal small particles. *JETP Letters*. 2013;97(9): 513–516.
28. Alam MJ, Tsuji M, Matsunaga M, Yamaguchi D. Shape changes in Au–Ag bimetallic systems involving polygonal Au nanocrystals to spherical Au/Ag alloy and excentered Au core Ag/Au alloy shell particles under oil-bath heating. *CrystEngComm*. 2011;13(8): 2984–2993.
29. Yasnikov IS. The formation of regions free of twin boundaries at the periphery of electrolytic pentagonal small particles. *Technical Physics Letters*. 2014; 40: 411–413.
30. Dorigin LM, Kolesnikova AL, Romanov AE. Misfit layer formation in icosahedral nanoparticles. *Technical Physics Letters*. 2008;34: 779–781.
31. Gutkin MY, Panpurin SN. Equilibrium ensembles of quantum dots in atomically inhomogeneous pentagonal nanowires. *Physics of the Solid State*. 2014;56: 1187–1194.

32. Gutkin MY, Kolesnikova AL, Krasnitckii SA, Dorogin LM, Serebryakova VS, Vikarchuk AA, Romanov AE. Stress relaxation in icosahedral small particles via generation of circular prismatic dislocation loops. *Scripta Materialia*. 2015;105: 10–13.
33. Gutkin MY, Kolesnikova AL, Yasnikov IS, Vikarchuk AA, Aifantis EC, Romanov A E. Fracture of hollow multiply-twinned particles under chemical etching. *European Journal of Mechanics-A/Solids*. 2018;68: 133–139.
34. Krauchanka MY, Krasnitckii SA, Gutkin MY, Kolesnikova AL, Romanov AE. Circular loops of misfit dislocations in decahedral core-shell nanoparticles. *Scripta Materialia*. 2019;167: 81–85.
35. Krauchanka MY, Krasnitckii SA, Gutkin MY, Kolesnikova AL, Romanov AE. Circular loops of misfit dislocations in decahedral core-shell nanoparticles. *Scripta Materialia*. 2019;167: 81–85.
36. Vlasov NM, Lyubov BY. Spreading of a finite low-angle tilt boundary due to non-conservative motion of dislocations. *Sov. Physics of Metals and Metallurgy*. 1975;40(6): 1162–1168.
37. Lyubov BY, Vlasov NM. Sov. Some effects of interaction between point and extended defects. *Physics of Metals and Metallurgy*. 1979;47(1): 140–157.
38. Vlasov NM, Lyubov BYa. Impurity atmosphere condensation at the wedge disclination. *Reports of the USSR Academy of Sciences*. 1981;259(2): 348–351.
39. Mikhailin AI, Romanov AE. Amorphization of disclination core. *Sov. Physics of the Solid State*. 1986; 28(2): 601–603.
40. Romanov AE, Samsonidze GG. Diffusion in the elastic field of a wedge disclination. *Sov. Technical Physics Letters*. 1988;14(14): 585–586.
41. Osipov AV, Ovid'ko IA. Diffusion-induced decay of disclinations and solid state amorphization in mechanically alloyed materials. *Applied Physics A*. 1992;54: 517–519.
42. Nazarov AA. Grain-boundary diffusion in nanocrystals with a time-dependent diffusion coefficient. *Physics of the Solid State*. 2003;45: 1166–1169.
43. Murzaev RT, Nazarov AA. Energies of formation and activation for migration of grain-boundary vacancies in a nickel bicrystal containing a disclination. *The Physics of Metals and Metallography*. 2006;102: 198–204.
44. Nazarov AA, Murzaev RT. Computer simulation of the interaction of junction disclinations in nanomaterials with grain boundary vacancies. *Solid State Phenomena*. 2008;137: 1–8.
45. Kolesnikova AL, Gutkin MY, Proskura AV, Morozov NF, Romanov AE. Elastic fields of straight wedge disclinations axially piercing bodies with spherical free surfaces. *International Journal of Solids and Structures*. 2016;99: 82–96.
46. Krasnitckii SA, Gutkin MY, Kolesnikova AL, Romanov AE. Formation of a void as stress relaxation mechanism in decahedral small particles. *Letters on Materials*. 2022;12(2): 137–141.
47. Vlasov NM, Zaznoba V. Diffusion processes near triple joints of special grain boundaries. *Physics of the Solid State*. 1999;41: 55–58.
48. Vlasov NM, Fedik II. Hydrogen segregation in the area of threefold junctions of grain boundaries. *International Journal of Hydrogen Energy*. 2002;27(9): 921–926.
49. Vlasov NM, Fedik II. Diffusion-induced relaxation of residual stresses. *Doklady Physics*. 2000; 45(11): 623–626.
50. Vlasov NM, Dragunov YG. Phase transformations in pentagonal nanocrystals. *Technical Physics*. 2013;58: 218–222.
51. Vlasov NM, Dragunov YG. Formation of zirconium hydride in the vicinity of stereo disclinations. *Technical Physics*. 2013;58(6): 892–895.
52. Vlasov NM, Zaznoba VA. Kinetics of migration (deposition) of fission products and interstitial impurities to sinks with different singularities. *Physics of the Solid State*. 2014;56(3): 518–521.
53. Tsagrakis I, Yasnikov IS, Aifantis EC. Gradient elasticity for disclinated micro crystals. *Mechanics Research Communications*. 2018;93: 159–162.

54. Khramov AS, Krasnitckii SA, Smirnov AM, Gutkin M. The Void Evolution Kinetics driven by residual stress in icosahedral particles. *Material Physics and Mechanics*. 2022;50(3): 401–409.
55. Podolyan OM, Zaporozhets TV. Void formation and collapse in nanowires. *Ukrayins'kij Fizichnij Zhurnal*. 2011;56(9): 933–943.

THE AUTHORS

Khramov A.S. 

e-mail: 242531@niuitmo.ru

Krasnitckii S.A. 

e-mail: Krasnitsky@inbox.ru

Smirnov A.M. 

e-mail: andrei.smirnov@niuitmo.ru

Gutkin M.Yu. 

e-mail: m.y.gutkin@gmail.com